

Hirshfeld Surface Analysis, DFT Studies, Docking Studies and Antimicrobial Activities of Cobalt Complex of Triple Sulfa Drugs Constituent Sulfamerazine with Secondary ligand Pyridine

Rahul P. Dubey¹, Urmila H. Patel²

Research Student, Department of Physics, Sardar Patel University, V.V.Nagar, Gujarat, India¹

Professor, Department of Physics, Sardar Patel University, V.V.Nagar, Gujarat, India²

ABSTRACT: Bond length and bond angles of cobalt complex of sulfamerazine with secondary ligand pyridine have been calculated by using B3LYP* method and compared with X-ray data. Molecular properties such as Homo-Lumo energy and NBO analysis of cobalt complex of sulfamerazine with secondary ligand pyridine have been studied by DFT method. Charges on atom are calculated by Mulliken population analysis and Natural population analysis. From Hirshfeld surface analyses, important intermolecular interactions are identified. The molecular docking studies concede that proposed molecule have high E-value with 13GS receptor. The antimicrobial and antifungal activities of synthesized complex and free ligand are performed.

KEYWORDS: Co complex of Sulfamerazine, NBO, MPA & NPA, Homo-Lumo, Molecular docking, Antimicrobial and antifungal activity.

I. INTRODUCTION

Sulfamerazine (SMR) is one of the potent sulfonamides and is a typical example of this family of bacteriostatic drugs. Sulfamerazine, one of the triple sulfadrag is very effective anti-arthritis. In the search for novel drugs against chloroquine-resistant malaria parasites, the modification of existing drug by coordination to a metal center has attracted considerable attention recently [1-5]. The effectiveness of the SMR can be enhanced by coordinating with a suitable metal ion. Literature survey reveals that DFT studies and molecular docking of sulfonamide complexes have not been well studied so far. In our previous work, X-ray crystallographic studies of cobalt complex of sulfamerazine with secondary ligand pyridine have been published by us [6]. The cobalt complex of sulfamerazine crystallizes in monoclinic space group C2/c with lattice parameter $a = 41.9224(15)\text{\AA}$, $b = 11.0836(4)\text{\AA}$ and $c = 14.8909(5)\text{\AA}$ and $\beta = 100.970^\circ(1)$ with $Z = 8$ with two molecules of sulfamerazine along with two molecules of pyridine solvent per asymmetric unit, co-ordinate via cobalt atom.

However quantum chemical aspects of such molecule has not been fully evaluated and due to this fact the study of this important molecule needs to continue in order to provide new information about the stability, biological activity, molecular docking and quantum properties that lacks in the literature, thus increasing the knowledge about this important dynamic molecule. Firstly, the molecule is optimized by using Jaguar programme incorporated in Schrodinger software with B3LYP/LAV2P* basic set. The optimized molecule structure of cobalt complex of sulfamerazine with secondary ligand pyridine is shown in Figure 1.

Bond lengths and bond angles of the optimized geometry have been compared with X-ray data. Molecular properties like NBO, MPA and NPA charges and HOMO-LUMO energy have been studied. To understand the intramolecular interactions which are playing the crucial role in stabilizing the molecule, Natural Bond Orbital (NBO) analysis has

International Journal of Innovative Research in Science, Engineering and Technology

(A High Impact Factor & UGC Approved Journal)

Website: www.ijirset.com

Vol. 6, Issue 8, August 2017

been carried out by using B3LYP method. The charges on the atom in the molecule have been calculated by Mullikan population analysis and Natural population analysis. Homo and Lumo energy of the molecule have been calculated in order to understand the reactivity as well as stability of the molecule. In our research, we have selected different receptor which shows anti-HIV-1 activity. The receptors are docked with proposed molecule and the energy value obtained using 'HEX' software [7].

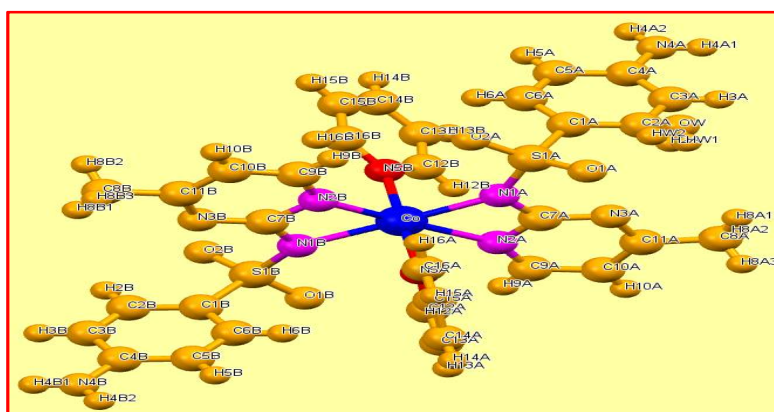


Figure 1 Optimized geometry of the molecule

In order to identify important intermolecular interactions within a crystal structure, Hirshfeld surface [8] of a title molecule has been calculated using CRYSTAL EXPLORER 2.1 [9-10]. With the best of our knowledge, neither Density functional theory nor Hirshfeld surface analysis and docking studies of proposed molecule are performed yet now.

In the present study, the synthesized complex is also studied by micro broth dilution method to understand its antimicrobial and antifungal activities.

II. COMPUTATIONAL DETAILS

All density function theory calculations have been performed by using computer software package Schrodinger [11]. The B3LYP (Becke three parameter Lee-Yang-Parr) [12-13] method with LAV2P* basis set are used to determine optimized geometry. The HEX software has been used for molecular docking studies. Hirshfeld surface of a title molecule has been calculated using CRYSTAL EXPLORER 2.1 in order to identify important intermolecular interactions within a crystal structure.

III. RESULTS AND DISCUSSION

3.1 Molecular geometry

An optimized bond lengths and bond angles are listed in Table 1 and these are compared with the crystalline data (X-ray). It has been observed that most of theoretical data (B3LYP) are fractionally higher than the crystalline data (X-ray). Theoretical data are calculated in the gaseous phase whereas the experimental data are calculated in solid state. The deviations in bond length between X-ray and B3LYP data for C1A-C2A, C1B-C2B and C4A-C5A in the phenyl ring are about 0.002Å, 0.016Å and 0.018Å respectively. The deviations in bond length for S1A-O1A and S1B-O1B are found out to be 0.124Å and 0.112Å respectively. The maximum deviations in bond length for non-hydrogen atom have been observed for S1B-N1B is about 0.146Å in the molecule. The deviations occur between B3LYP data and X-ray data are due to fact that hydrogen bond interactions are involved in the X-ray data which are not considered by B3LYP data. Also the surrounding crystal packing effects is playing a significant role in altering the X-ray and B3LYP data since it is the challenging task to model the crystal packing by simple DFT method. The deviations in bond angle depend on an electro negativity of the central atom and the presence of a lone pair of electrons. The deviations in bond angle C7B-N1B-Co and C7A-N1A-Co is about 11.31° and 7.55°.

International Journal of Innovative Research in Science, Engineering and Technology

(A High Impact Factor & UGC Approved Journal)

Website: www.ijirset.com

Vol. 6, Issue 8, August 2017

Table 1 Comparisons of bond length and bond angle of X-ray (Experimental) data with B3LYP Data (Theoretical).

Bond length (Å)						Bond angle(°)		
Atoms	X-ray (Å)	B3LYP (Å)	Atoms	X-ray (Å)	B3LYP (Å)	Atoms	X-ray (°)	B3LYP(°)
Molecule –A (Sulfamerazine)						Molecule –A (Sulfamerazine)		
S1A -O1A	1.444 (2)	1.549	C1A-C2A	1.392 (4)	1.390	O2A -S1A -O1A	116.27 (13)	118.568
S1A-N1A	1.598 (2)	1.745	C2A-C3A	1.385 (4)	1.389	N1A -S1A -O2A	105.31 (12)	101.695
S1A-O2A	1.440 (2)	1.561	C3A-C4A	1.376 (5)	1.408	C1A -S1A -O2A	108.59 (14)	106.351
S1A-C1A	1.752 (3)	1.843	C4A-C5A	1.390 (6)	1.408	N1A-S1A-O1A	112.00 (12)	112.845
N1A-C7A	1.369 (3)	1.361	C5A-C6A	1.392 (5)	1.390	C1A-S1A -O1A	107.24 (12)	108.165
N2A-C7A	1.358 (3)	1.364	C1A-C6A	1.390 (4)	1.389	C1A-S1A -N1A	107.06 (12)	108.673
N2A -C9A	1.337 (3)	1.329	C8A-C11A	1.491 (4)	1.506	C7A -N1A -S1A	122.28 (17)	121.389
N3A-C11A	1.343 (3)	1.340	C9A-C10A	1.379 (4)	1.394	C9A -N2A -C7A	116.2 (2)	116.806
N3A-C7A	1.327 (3)	1.344	C10A-C11A	1.376 (4)	1.400	C11A-N3A -C7A	116.6 (2)	116.845
N4A-C4A	1.378 (4)	1.389				C2A -C1A -S1A	120.5 (2)	119.652
Molecule –A (Pyridine)						Molecule –A (Pyridine)		
N5A -C12A	1.327 (4)	1.343	C13A -C14A	1.372 (4)	1.395	C13A -C12A-N5A	123.0 (3)	121.938
N5A -C16A	1.334 (3)	1.342	C14A -C15A	1.368 (5)	1.392	C14A -C13A -C12A	119.5 (3)	118.790
C12A -C13A	1.371 (4)	1.391	C15A -C16A	1.373 (4)	1.393	C15A -C14A -C13A	118.3 (3)	118.971
Molecule –B (Sulfamerazine)						Molecule –B (Sulfamerazine)		
S1B-O1B	1.437 (2)	1.561	C1B -C2B	1.374 (4)	1.390	O2B -S1B -O1B	115.59 (13)	118.557
S1B-N1B	1.599 (2)	1.745	C2B-C3B	1.372 (5)	1.389	N1B -S1B -O2B	112.46 (14)	112.856
S1B-O2B	1.444 (2)	1.549	C3B -C4B	1.380 (5)	1.408	C1B -S1B -O2B	106.94 (13)	108.225
S1B-C1B	1.766 (3)	1.844	C4B -C5B	1.381 (5)	1.407	N1B -S1B -O1B	104.85 (12)	101.713
N1B-C7B	1.373 (3)	1.361	C5B -C6B	1.384 (5)	1.390	C1B -S1B -O1B	108.95 (14)	106.276
N2B-C7B	1.356 (4)	1.365	C1B -C6B	1.382 (4)	1.389	C1B -S1B -N1B	107.81 (13)	108.661
N2B-C9B	1.339 (4)	1.329	C8B -C11B	1.496 (4)	1.506	C7B -N1B -S1B	123.19 (18)	121.394
N3B-C11B	1.357 (4)	1.340	C9B -C10B	1.353 (4)	1.395	C9B -N2B -C7B	117.5 (2)	116.805
N3B-C7B	1.333 (3)	1.344	C10B-C11B	1.375 (5)	1.400	C11B -N3B -C7B	114.9 (3)	116.863
N4B-C4B	1.376 (4)	1.386				C2B -C1B -S1B	121.0 (2)	119.668
Molecule –B (Pyridine)						Molecule –B (Pyridine)		
N5B -C12B	1.324 (4)	1.342	C13B -C14B	1.357 (5)	1.392	C13B -C12B -N5B	124.3 (3)	121.825
N5B -C16B	1.337 (4)	1.343	C14B -C15B	1.364 (6)	1.395	C14B -C13B -C12B	119.1 (3)	118.911
C12B-C13B	1.373 (5)	1.393	C15B -C16B	1.369 (6)	1.391	C15B -C14B -C13B	118.3 (4)	118.966
Co-ordination around of cobalt								
Co-N1A	2.103 (2)	2.060	Co -N1B	2.165 (2)	2.059			
Co-N5A	2.171 (2)	2.049	Co-N5B	2.181 (2)	2.108			

3.2 Molecular properties

3.2.1 NBO analysis

Natural bond orbital (NBO) [18] calculations are performed using Jaguar program as built in the Schrodinger package software at B3LYP/LAV2P* level of theory. This method provides the resourceful way for studying intra molecular bonding and interactions between bonds. For investigating the rate of charge transfer between molecular systems, this method can be useful. The stabilization energy $E^{(2)}$ associated with $i(\text{donor}) \rightarrow j(\text{acceptor})$ delocalization is estimated from a second order perturbation approach as given below and tabulated in Table 2.

$$E^{(2)} = \Delta E_{NL,L} = q_i (F(L,NL) / E(NL) - E(L))$$

Where q_i is a donor orbital occupancy $E(NL), E(L)$ are diagonal elements (orbital energies) and $F(L,NL)$ is the off-diagonal NBO Fock matrix element. Greater $E^{(2)}$ values displays the more intensive in the interaction between electron donors and electron acceptors, which explain the more donating tendency from electron donors to electron acceptors and the greater extent of conjugation of the whole system. The most interesting intermolecular interaction has been found between lone pair of N1B with that of antibonding Co. The interaction energy between these bonding and antibonding orbital is about 37.35Kcal/mol. The intermolecular interaction energy (stabilizing energy) between lone pair N1A and antibonding N2A-C7A is 26.54Kcal/mol. The stabilizing energy between lone pair N5B and antibonding cobalt is 21.24Kcal/mol. The intense energy has been found between N3B-C11B and N2B- C7B with the stabilizing energy value of about 22.32Kcal/mol.

International Journal of Innovative Research in Science, Engineering and Technology

(A High Impact Factor & UGC Approved Journal)

Website: www.ijirset.com

Vol. 6, Issue 8, August 2017

Table 2 Stabilization energy $E^{(2)}$ associated with i (donor) \rightarrow (acceptor) delocalization is estimated from a second order perturbation approach

Donor (L) NBO	Acceptor (NL) NBO	E(2) kcal/mol	E(2) E(NL)-E(L)	F(L,N L)	Donor (L) NBO	Acceptor (NL) NBO	E(2) kcal/mol	E(2) E(NL)-E(L)	F(L,NL)
LP (1) N1A	LV (5)Co	11.24	0.24	0.065	BD (2) C9A- C10A	BD*(2) N3A- C11A	19.56	0.25	0.089
LP (1) N1A	LV (6)Co	16.59	1.37	0.19	LP (1) N1B	LV (5)Co	11.5	0.23	0.065
LP (2) N1A	LV (5)Co	33	0.05	0.05	LP (1) N1B	LV (6)Co	16.5	1.36	0.189
LP (2) O1A	BD*(1) S1A- C1A	7.77	0.45	0.074	LP (2) N1B	LV (5)Co	37.35	0.04	0.05
LP (3) O1A	BD*(1) S1A- O2A	8.7	0.5	0.083	BD (2) N5B- C12B	BD*(2) C15B- C16B	13.33	0.32	0.083
LP (3) O1A	BD*(1) S1A- N1A	7.12	0.42	0.069	BD (2) C 68- C14B	BD*(2) N5B- C12B	15.91	0.26	0.081
LP (2) O2A	BD*(1) S1A- N1A	6.11	0.43	0.065	BD (2) N5A- C 62	BD*(2) C15A- C16A	13.92	0.33	0.085
LP (2) O2A	BD*(1) S1A- C1A	4.84	0.46	0.059	BD (2) C13A-C14A	BD*(2) N5A- C 62	17.32	0.24	0.082
LP (3) O2A	BD*(1) S1A- O1A	9.23	0.51	0.087	BD (2) C13A-C14A	BD*(2) C15A- C16A	9.25	0.27	0.063
LP (2) N1A	BD*(2) N2A- C7A	26.54	0.24	0.1	BD (2) C15A-C16A	BD*(2) N5A- C 62	8.57	0.25	0.059
LP (1) N2A	BD*(1) N3A- C7A	6.25	0.88	0.093	BD (2) C15A-C16A	BD*(2) C13A- C14A	12.35	0.29	0.075
LP (1) N 14	BD*(2) C3A- C4A	16.35	0.32	0.092	LP (1) N5B	LV (5)Co	21.24	0.18	0.079
BD (2) N2A- C7A	BD*(2) C9A- C10A	17.47	0.33	0.096	LP (1) N5B	LV (6)Co	20.55	1.32	0.208
BD (2) N3A- C11A	BD*(2) N2A- C7A	22.75	0.28	0.101	BD (2) C 9B- C10B	BD*(2) N3B- C11B	17.97	0.28	0.089
BD (2) C1A- C2A	BD*(2) C3A- C4A	7.86	0.27	0.059	BD (2) C3B- C4B	BD*(2) C1B- C2B	14.97	0.27	0.08
BD (2) C1A- C2A	BD*(2) C5A- C6A	13.72	0.28	0.078	BD (2) C3B- C4B	BD*(2) C5B- C6B	7.97	0.29	0.06
BD (2) C3A- C4A	BD*(2) C1A- C2A	14.52	0.28	0.08	BD (2) C5B- C6B	BD*(2) C1B- C2B	8.94	0.26	0.061
BD (2) C3A- C4A	BD*(2) C5A- C6A	8.38	0.27	0.06	BD (2) C5B- C6B	BD*(2) C3B- C4B	13.13	0.27	0.075
BD (2) C5A- C6A	BD*(2) C1A- C2A	8.19	0.28	0.061	BD (2) N2B- C7B	BD*(2) C 9B- C10B	19.14	0.3	0.096
BD (2) C5A- C6A	BD*(2) C3A- C4A	12.53	0.28	0.075	BD (2) N3B- C11B	BD*(2) N2B- C7B	22.32	0.28	0.101
LP (2) N1B	BD*(2) N2B- C7B	29.61	0.21	0.1	LP (3) O1B	BD*(1) S1B- O2B	9.53	0.5	0.087

***BD(1) stands for σ -orbital and BD(2) stands for π -orbital

3.2.2 Charge analysis

The charges on the atom are calculated by two different methods i.e. one is the Mulliken population analysis [19] and another one is the Natural population analysis [20] by using B3LYP method with LAV2P* basic set and shown in Figure 2. From the Figure 2, it can be observed that all hydrogen atoms are having the positive charge. H4A1/2, H4B1/2 hydrogen is having the maximum positive charge in comparison to other hydrogen atoms. From crystallographic study, it has been observed that these hydrogen atoms are forming the strongest intermolecular hydrogen bond interactions. The maximum positive charge carried by the Sulphur atom in the whole molecule. The cobalt atom is also having the positive charge just after the Sulphur atom in the title molecule. The sulfonamides oxygen and nitrogen atom is having the maximum negative charge. In the phenyl ring, C4A and C4B is carrying the positive charge whereas the all other carbon atom is carrying the negative charge in this ring. In the pyrimidine ring, C7A/B, C9A/B, C11A/B is carrying the positive charge whereas C9A/B is carrying the negative charge. In the pyridine ring, C12A/B and C16A/B is having the positive charge and C13A/B, C14A/B, C15A/B is having the negative charge. Literature survey reveals that atomic charge will have influence on dipole moment, polarizability, electronic structure and many other properties of the molecule.

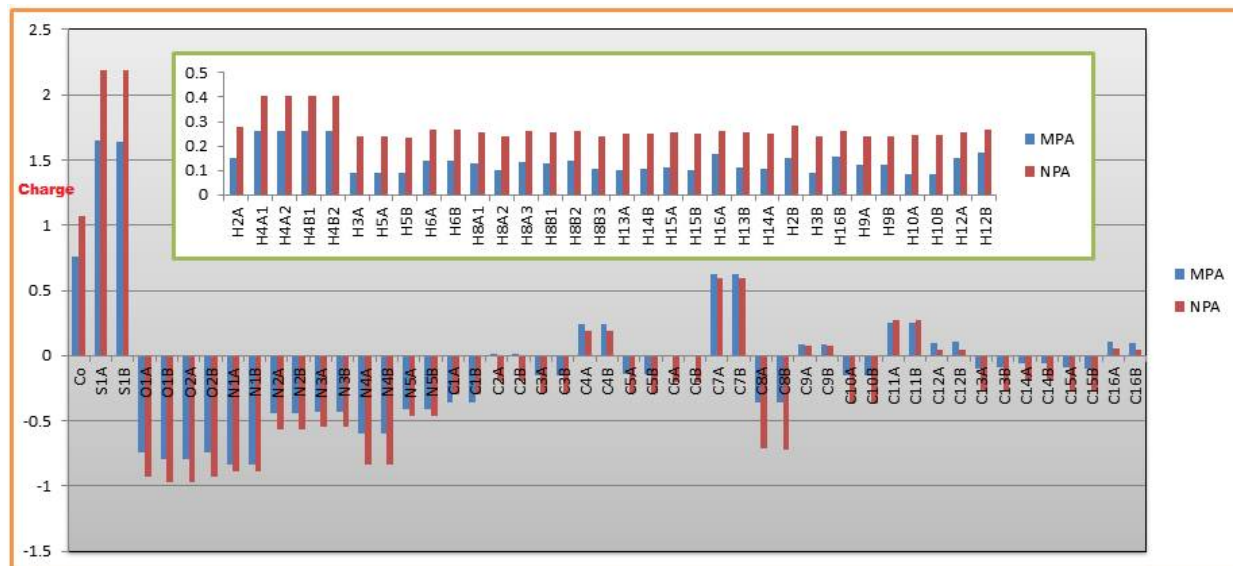


Figure 2 Charge on atom calculated by MPA and NPA analysis

3.2.3 HOMO and LUMO energy

HOMO and LUMO energy have been calculated by B3LYP method with basic set LAV2P* which is useful for understanding various aspects of pharmacological formulations including drug design and the possible Eco-toxicological characteristics of the drug molecules. In this molecule, the LUMO is localized on the cobalt atom and HOMO is localized on the Pyrimidine ring as well as on sulfonamidic nitrogen. The energies gap between HOMO and LUMO are about 3.18eV which explains the charge transfer interaction in the proposed molecule. The wider energy gap will explain the stability of the title molecule and it is pointing towards the harder molecule. The positive and negative phase represented in red and blue color respectively with HOMO and LUMO energy gap are shown in Figure 3. The calculated energy value of the HOMO-LUMO and the corresponding energy gaps along with quantum descriptors like Electro negativity, Chemical hardness, Electrophilicity index and Softness are listed in Table 3. The global hardness value of the molecule explains resistance towards the deformation of electron cloud of chemical systems during the chemical process [21-22].

Table 3 HOMO-LUMO and the corresponding energy gaps along with quantum descriptors

HOMO energy(eV)	LUMO energy(eV)	Energy gap(eV)		
-6.68	-3.50	3.18		
Hardness(η)	Softness(s)	Electronegativity (χ)	Electrophilicity index (ω)	Hardness(η)
-1.59(eV)	-0.63 (eV)	5.09(eV)	8.14(eV)	-1.59(eV)

International Journal of Innovative Research in Science, Engineering and Technology

(A High Impact Factor & UGC Approved Journal)

Website: www.ijirset.com

Vol. 6, Issue 8, August 2017

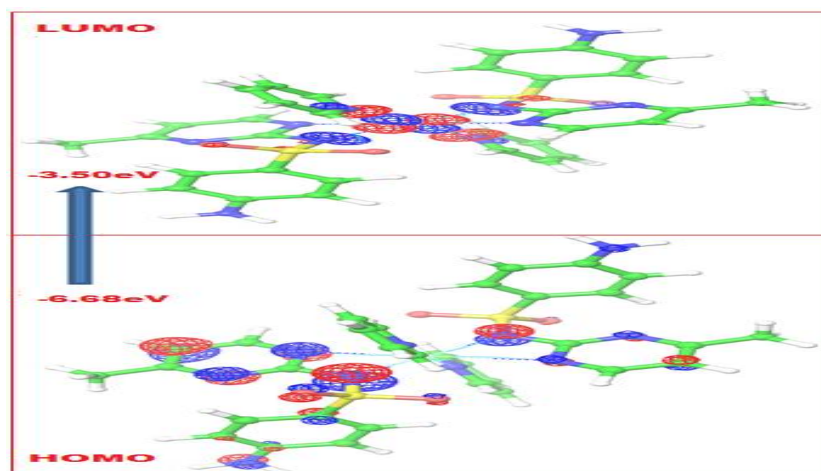


Figure 3 HOMO and LUMO energies

3.4 Hirshfeld surface energy

When the CIF file is read into the Crystal Explorer program for analysis, all bond lengths to hydrogen are automatically modified to typical standard neutron values (C–H = 1.083 Å and N–H = 1.009 Å). The 2-D fingerprint plots displayed by using the standard 0.6–2.8 Å view with the d_e and d_i distance scales displayed on the graph axes. The d_{norm} values are mapped onto the Hirshfeld surface by using a red–blue–white color scheme: where red regions correspond to closer contacts; the blue regions correspond to longer contacts and the white regions corresponding to the distance of contact is exactly equal to the r^{vdW} separation. D_{norm} surface and N–H...O interaction on the hirshfeld surface are shown in Figure 4. Figure 5 shows shape index and curvedness of the molecule. The red spot in D_{norm} surface shows closer N–H...O, C–H...O and O–H...O interactions. Shape index is the indicators of C–H... π interaction. In present molecule, C–H... π interaction has been found and shown in shape index (shown by circle) and it is characterized by red and blue triangle fronting each other. Curvedness surface is the indicator of π ... π stacking interaction. The small flat region (shown by square) observed on curvedness surface indicate existence of π ... π stacking interaction in present molecule. In the present molecule, pyridine ring take part in π ... π interaction. 2D finger plot and contribution of different interactions are shown in Figure 6 and 7 respectively. The H–H contacts cover most area in the 2-D fingerprint plots, have a most significant contribution to the total Hirshfeld surfaces (45.2%). The proportion of N–H/H–N contacts comprising 8.4% of the total Hirshfeld surfaces. The H–O contacts are characterized by distinct spikes. The proportion of O–H/H–O contacts comprising 20.2% of the total Hirshfeld surfaces for each molecule of the compound. The C–C contact in fingerprint plot is presented as characteristic stacking kite, which is mainly assigned to π – π interaction. The C–C contact includes only 1.2% of the total Hirshfeld surfaces area. At bottom left of the fingerprint plot, there are characteristic “wings” which are identified as a result of H–C contacts. The decomposition of the fingerprint plot shows that C–H/H–C contacts comprise 24.2% of the total Hirshfeld surface area. The other contacts like are only about 1.7% in the total Hirshfeld surfaces. So hirshfeld surface is very useful to visualize the hydrogen bond interaction and contribution of each interaction in the crystal packing which could be very useful in crystal engineering field.

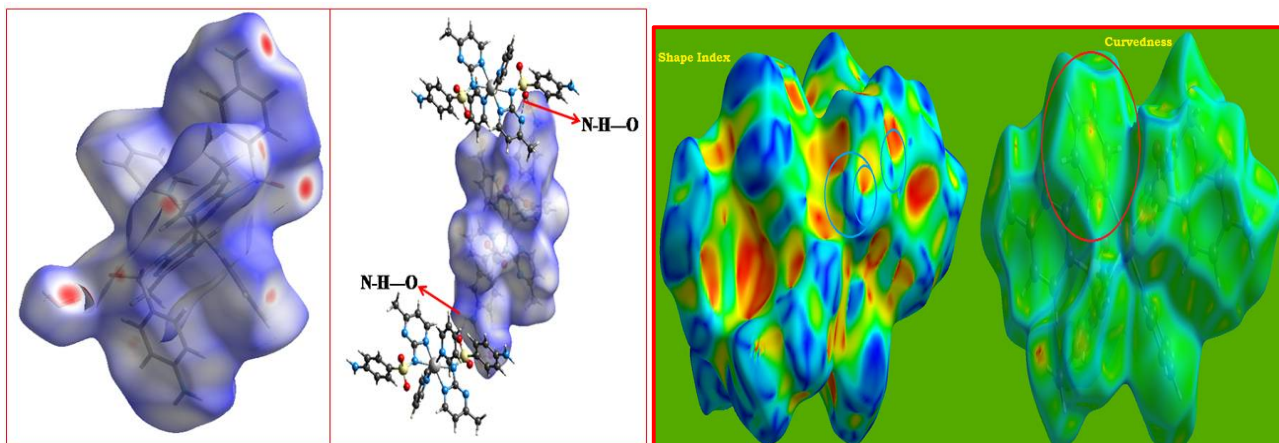


Figure 4 D_{norm} surfaces and N-H...O interaction Figure 5 Shape index and Curvedness of molecule

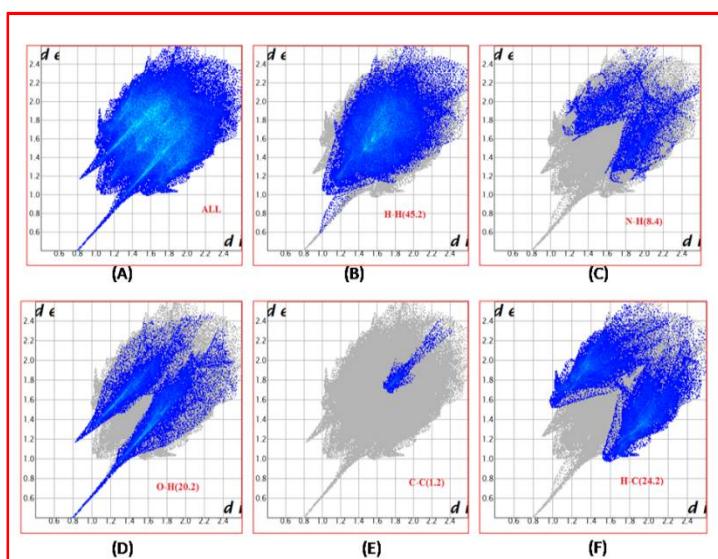


Figure 6 Finger plot

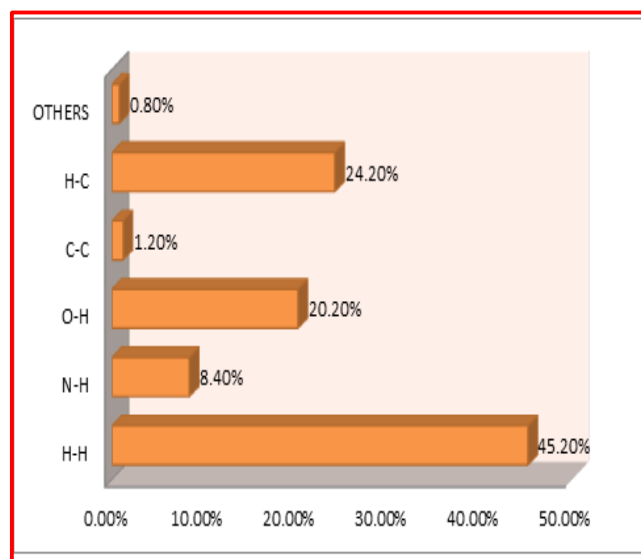


Figure 7 Interactions contribution

3.5 Molecular Docking

Computational biology and bioinformatics are useful for the drugs recovery process which reduces the cost of drugs. Rational Drug Design is the inventive process of finding new medications based on the knowledge of the biological target. Molecular docking predicts the strength of the binding, the energy of the ligand-receptors complex. Computer Aided Drug Design (CADD) is a specialized discipline for the study of simulation of ligand- receptor interactions and is strongly dependent on bioinformatics tools, applications and databases. The corresponding cif file has been converted into PDB file using OBGUI software. This PDB structure has been used for the docking studies using Hex software [27-28]. The receptor proved to be the best inhibitor of the ligand when ligand-receptor docks each other well. The title compound has been docked with the different receptors. The cobalt complex of sulfamerazine with secondary ligand pyridine is docked with few selected receptors. The parameters used for the docking process were

Correlation type - Shape only

FFT Mode - 3D fast lite

Grid Dimension - 0.6

International Journal of Innovative Research in Science, Engineering and Technology

(A High Impact Factor & UGC Approved Journal)

Website: www.ijirset.com

Vol. 6, Issue 8, August 2017

Receptor range – 180

Ligand range – 180

Twist range – 360

Distance Range – 40

The molecule is docked with receptor such as 13GS, 2Y5S, 1OKL, 4J7X, 1AZM, 4ITO, 4LHIT having E-value equal to -303.7, -285.1, -259.0, -264.9, -248.3, -266.9, -280.17 respectively. This E-value of docking of the Ligand with Receptor is shown in Figure 9. The title compound having highest interaction energy with 13GS receptors with energy values -303.74 and shown in Figure 8, which means that it was more compatible with receptor 13GS compare to other analogous.

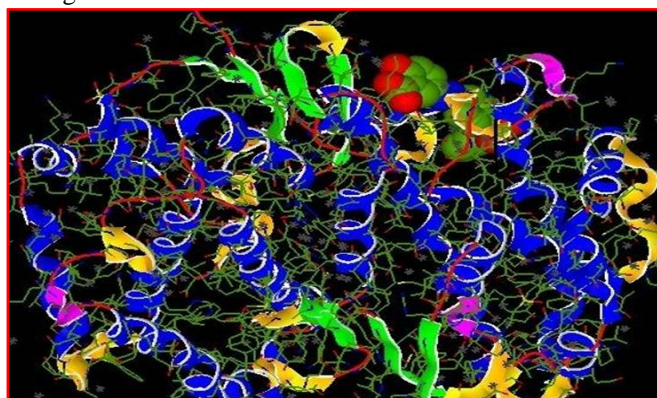


Figure 8 Docking of the Ligand with Receptor



Figure 9 E-value of docking of the Ligand with Receptor

3.6 Antimicrobial and Antifungal activity

The compound is synthesized by reflux method. In methanolic solution of sulfamerazine, aqueous solution of cobalt acetate is added dropwise. The precipitate was collected and washed several time with distilled water. The synthesized powder of sulfamerazine is again reflux with pyridine solvent. In this way, cobalt complex of sulfamerazine with pyridine solvent has been synthesized.

Antibacterial and antifungal activity of sulfamerazine and cobalt complex of sulfamerazine are compared and shown in Figure 10. Antibacterial and antifungal activity of synthesized complex of sulfamerazine and free sulfamerazine are evaluated by using micro broth dilution method [29-30]. Our observation reveals that cobalt complex of sulfamerazine is more effective against *SH. Flexneri* (gram positive) and *B.SUBTILLIS* (gram negative) than free sulfamerazine. The importance of cobalt complex is that it could be rationally used for the treatment of some common diseases caused by these bacteria. As it is known fact that gram-negative bacteria used in both clinical and experimental tumour chemotherapy and so this complex is better than free ligand. Our complex is tested against fungi such as *C.ALBICANS* and it has been observed that the complex and free ligand is having same strength against *C.ALBICANS* fungi.

International Journal of Innovative Research in Science, Engineering and Technology

(A High Impact Factor & UGC Approved Journal)

Website: www.ijirset.com

Vol. 6, Issue 8, August 2017

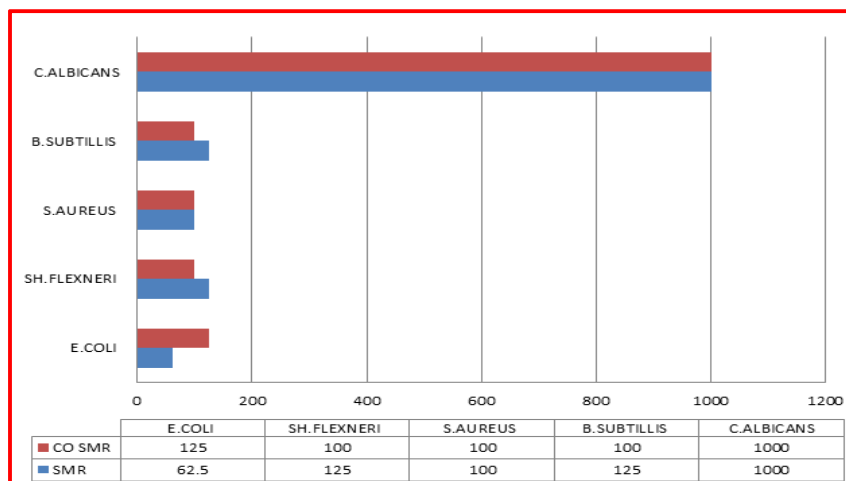


Figure 10 Antimicrobial and Antifungal activities of Sulfamerazine and its cobalt sulfamerazine

IV. CONCLUSION

Small deviations have been observed between X-ray data and B3LYP data and it is due to presence of good number of hydrogen bond interactions in X-ray data. From Hirshfeld surface, it can be observed that H-H contacts is playing important role in hydrogen bond interaction. Also, π - π and C-H... π interaction can be visualized from the curvedness and shape index of the molecule. Docking studies reveals that, proposed molecule having highest interaction energy with 13GS receptors. From antimicrobial activity, it can be observed that cobalt complex of sulfamerazine is more effective against SH. Flexneri (gram positive) and B.SUBTILLIS (gram negative) than free sulfamerazine.

ACKNOWLEDGEMENTS

We are very much thankful to DST- FIST, New Delhi for funding towards Schrodinger software under UGC-DSA facility, at Department of Physics, Sardar Patel University, Vallabh Vidyanagar, Gujarat, India.

REFERENCES

- [1] M Wisniewski, A Opolski, J Wietrzyle, J. INORG.BIOCHEM, 86, 480(1987).
- [2] J Pranata, SG Wierschkajorgenson, J.AM. CHEM. SOC, 1132, 810(1991).
- [3] M Navarro, EJ Cisnero-Fajardo, T lehmann, RA Sanchez-Delgado, R atencio, P Silvia, R Lira, JA urbina; J.INORG. CHEM.,40, 6879(2001).
- [4] R Robin, M Coombs, K Ringer, JM Blacquire, J C Smith, J Scottneilsen, Trans.Met.Chem, 30, 411(2005).
- [5] NH Gokhale, SB padhye, S L croft, HD kendrick, W davies, CE anson, AK Powell, J. INORG. BIOCHEM. 95, 249(2003).
- [6] Tailor, Sanjay; Dubey, Rahul; Patel, Urmila, LAP LAMBERT Academic Publishing, ISBN 13:9783659618956(2014).
- [7] HexServer: an FFT-based protein docking server powered by graphics processors. G. Macindoe, L. Mavridis, V. Venkatraman, M.-D. Devignes, D.W. Ritchie (2010).
- [8] M.A. Spackman, D. Jayatilaka, CrystEngCom., 11, 19-32(2009)
- [9] S.K. Wolff, D.J. Grimwood, J.J. McKinnon, M.J. Turner, D. Jayatilaka, M.A. Spackman, University of Western Australia, 2012.
- [10] M.A. Spackman, J.J. McKinnon, CrystEngComm, 4, 378-392(2002).
- [11] A. D. Bochevarov, E. Harder, T. F. Hughes, J. R. Greenwood, D. A. Braden, D. M. Philipp, D. Rinaldo, M. D. Halls, J. Zhang, R. A. Friesner International Journal of Quantum Chemistry, 113, 2110(2013).
- [12] B G Jhonson, P M Gill and J A Pople, The Journal of Chemical Physics, 98, 5612(1993).
- [13] C Lee, W Yang and R G Parr, Physical Review B, B37, 785-789 (1988).
- [14] Yang W, Parr RG. Hardness, softness, and the Fukui function in the electronic theory of metals and catalysis. ProcNatiAcadSci USA,82:6723-6726(1985).
- [15] M. Oftadeh, N. MadadiMahani, and M. Hamadani, Res Pharm Sci, 8(4): 285-297(2013).
- [16] Faver J, Merz KM. Utility of the hard/soft acid-base principle via the Fukui function in biological systems. J Chem Theory Comput. 6:548-559(2010).
- [17] Kathy Ramirez-Balderrama, ErasmoOrrantia-Borunda, Norma Flores-Holguin, Journal of Theoretical and Computational Chemistry, Vol. 16, No. 03(2017).

International Journal of Innovative Research in Science, Engineering and Technology

(A High Impact Factor & UGC Approved Journal)

Website: www.ijirset.com

Vol. 6, Issue 8, August 2017

- [18] M. Szafran, A. Komasa, E.B. Adamska, J. Mol. Struct. Theochem., 827, 101-107(2007).
- [19] Mulliken, R. S. "Electronic Population Analysis on LCAO-MO Molecular Wave Functions. I". The Journal of Chemical Physics. 23 (10): 1833-1840(1955).
- [20] Alan E. Reed, Robert B. Weinstock, and Frank Weinhold, The Journal of Chemical Physics 83, 735(1985).
- [21] K. Govindarasu, E. Kavitha, Journal of Molecular Structure, 1088, 70-84 (2015).
- [22] Diego M. Gil, M.E. DefonsiLestard, O.Estévez-Hernández, J. Duque, E. Reguera, Spectrochimica Acta Part A: Molecular and Biomolecular Spectroscopy, 145, 553-562(2015).
- [23] Lewis RA "Chapter 4: The Development of Molecular Modeling Programs: The Use and Limitations of Physical Models". In Gramatica P, Livingstone DJ, Davis AM. Drug Design Strategies: Quantitative Approaches. Royal Society of Chemistry, 88-107(2011).
- [24] Rajamani R, Good AC, Current Opinion in Drug Discovery & Development,10(3),308-15(2007).
- [25] N.S. Labidi, A. Djebaili, I. Rouina, Journal of Saudi Chemical Society,15, 29-37(2011).
- [26] D. Kleinman, J. Phys. Rev, 126, 1977-1979 (1962).
- [27] The Protein Data Bank, Nucleic Acids Research, Vol. 28, Oxford University Press, 2000.
- [28] U.H Patel, R. A. Barot, B. D. Patel, D. A. Shah, R. D. Modh, International Journal of Environmental Science, Volume 2, No 1, (2011).
- [29] National Committee for Clinical Laboratory Standards, Methods for Dilution Antimicrobial Susceptibility Tests for Bacteria that grow aerobically, approved standard, M7A5, fifth ed., National Committee for Clinical Laboratory Standards: Wayne, PA, (2000).
- [30] Gehad, G.M., Mohamed, M.O. and Ahmed, M.H., Journal of Chemistry, 30, 361-382(2006).